KSCE Journal of Civil Engineering (2024) 28(2):849-859
DOI 10.1007/s12205-023-1043-7

pISSN 1226-7988, eISSN 1976-3808
www.springer.com/12205

Structural Engineering

Fatigue Life Comparison of Tubular Joints in Tripod and Jacket Offshore Support Substructures Using 3D Fatigue FE Analysis

Shazia Muzaffer[a], **Kyong-Ho Chang**[b], **and Mikihito Hirohata**[c]

[a]*Dept. of Civil, Environmental & Plant Engineering, Chung-Ang University, Seoul 0697, Korea*
[b]*Member, Dept. of Civil, Environmental & Plant Engineering, Chung-Ang University, Seoul 0697, Korea*
[c]*Dept. of Civil Engineering, Osaka University, 565-0871, Osaka, Japan*

ARTICLE HISTORY

Received 19 May 2023
Accepted 2 November 2023
Published Online 28 December 2023

KEYWORDS

Fatigue FE
Fatigue crack initiation
Offshore structures
Continuum mechanics
Constitutive equations
Fatigue life

ABSTRACT

In a wind energy system, the safety and stability of substructures plays an important role during the in service of offshore structure. Offshore structures are continuously subjected to high cyclic fatigue loads and may experience fatigue cracks due to the continuous accumulation of plastic strain and stress concentrations at welded joints. The fatigue life of welded tubular joints is one of the most important factors determining the life of offshore structures. In this study, the fatigue analysis of tubular joints of the tripod and jacket support structure was performed using 3D fatigue FEM to estimate the fatigue life and predict the positions of crack initiation. The 3D fatigue FE is based on constitutive equations and continuum damage mechanics. The welding state of tubular joints were reproduced to calculate the welding residual stresses and welding deformation. The residual stresses and weld deformation were used as input together with cyclic loading in the 3D fatigue FE to calculate the fatigue life and predict the crack initiation positions. The S-N curve calculated by the 3D fatigue FE analysis were compared with the SN curves of Eurocode 3. The results show that 3D fatigue FE analysis is an effective tool to analyze large and complex structures before installation to ensure the safety and stability of the structure.

1. Introduction

Offshore wind energy is a continuously renewable source of energy that does not produce harmful greenhouse gas emissions. An increase in energy from offshore wind helps the world reduce CO2. The volume of offshore wind turbines installed annually is expected continuously to increase in order to achieve net zero gas emissions by 2050. Wind turbines system consist of structural members (main parts) and a series of mechanical and electrical components with a control system. The main structural members of a wind turbine consist of a tower and a substructure member. The tower is made of a conical steel cross-section, and the mechanical parts of the wind turbine are attached to the top of the tower. The tower rests on the top of the substructure, which is anchored to piles that are fixed in the ground. The installation, operation, and maintenance of offshore wind turbines require consideration of various aspects related to the design, safety, and stability of the structure. The current trend is to install large wind turbines of 6 MW or more in deeper waters, which increases the requirements for efficient substructure design. Currently, different types of substructures are installed around the world depending on certain aspects such as water depth, seabed geology, and sea state conditions. Fabrication, installation, and maintenance of fixed offshore substructures are economical compared to floating offshore substructures. Monopiles and lattice structures are the most common fixed offshore support structures. Monopiles are widely used in shallow waters due to the relative simplicity of fabrication and installation. However, extending the monopiles in deep water depths need more material tonnage to assure performance, and installation becomes expensive. When the water depth is more than 50 m, the tripod is sturdier than the monopile and easier to manufacture. The tripod structures are supported by three legs diverging from a central node configured in an equilateral triangle, the upper part of which supports the central steel column mounted with a tower and the lower part of which is connected to the seabed by piles. However, in water

CORRESPONDENCE Kyong-Ho Chang changkor@cau.ac.kr Dept. of Civil, Environmental & Plant Engineering, Chung-Ang University, Seoul 0697, Korea

depths greater than 100 m, the jacket substructure has proven to be an efficient support structure due to its high overturning resistance, greater structural stiffness, and convenient and efficient offshore installation. The substructures are constantly subjected to external static or cyclic loads such as environmental loads, dead loads, and repeated loads in addition to operational loads. The severe cyclic environmental loads during the operational period cause plastic stresses that may result in initial fatigue cracks. Under sustained cyclic loading, the accumulation of plastic strains alters the mechanical behavior of the material, which in turn accelerates crack propagation and eventually leads to catastrophic failures. Engineers involved in efficient design and construction are fully aware that offshore substructures need to be designed with care as the stability of the whole structure is governed by substructures. Several experimental studies were conducted, but they were costly, time-consuming, and complicated. Various numerical tools were used by different researchers to accurately estimate the fatigue life of offshore substructures. To calculate the fatigue life and crack initiation of tubular joints of jacket and tripod support structure, 3D fatigue FE analysis based on constitutive equations and continuum damage mechanics was used. This study enables a direct comparison of the fatigue life of tubular joints in offshore substructures and predicts crack initiation positions.

2. Literature Review

Sadeghi (2007) summarized the general understanding of the various aspects and stages of design, transportation, construction, loading, and installation of different types of offshore structures. Kharade and Kapadiya (2014) discussed the accurate prediction and estimation of important forces that contribute to the stable and safe design of offshore structures. Oh et al. (2018) and Ashuri and Zaaijer (2007) provided an overview of basic concepts, design methods, challenges, and current and future trends in various foundations. They also explained the advantages, disadvantages, limitations, and static and dynamic behavior of soils over short and long periods for each foundation type. Chew et al. (2013, 2014) conducted a comparative study between a three-legged and a four-legged design and concluded that the three-legged design was feasible and economical, saving 17% of the total structural mass required and reducing the number of welds by 25%. The performance of the four and three-legged jacket structures with respect to different load cases, wind wave displacement, and loading direction was investigated. Zaaijer (2003) studied the comparison of the properties of monopile, tripod, suction bucket, and gravity base for a 6 MW turbine. Henderson et al. (2003) studied the hydrodynamic loading of offshore structures, investigated different recommendations for slender (monopiles) and compact (GBS) structures, and analyzed the design methods that consider the effects of stochastic nonlinear waves on the structures in shallow waters. Mayilvahanan Alagan Chella et al., (2012) provided an overview of the effect of breaking waves on the substructures of offshore wind turbines and the corresponding responses of the structure to wave impact forces. The tripod pile is more advantageous than monopiles due to its lighter weight and quick installation, so it is used in many locations with extreme and prolonged waves. The dynamic coupled analysis with soil-pile interactions for an NREL 5MW OWT supported by a tripod structure was carried out to demonstrate the higher efficiency and accuracy of pile-support structures should be used in the design of offshore structures (Plodpradit et al., 2019). Afandi and Muis Alie (2020) performed a numerical analysis to predict the fatigue life of jacket structures subjected to axial and wave loading. In the dynamic analysis, higher damage was predicted due to higher stresses, and the most affected joints were located at the diagonals of the jacket substructures (Mendes et al., 2021). Stahlmann and Schlurmann (2010) examined the scour phenomena around complex foundations tripod and investigated the effects of scour on the stability and durability of the structure. Yang et al. (2015) studied reliability-based design optimization under dynamic constraints for a sub-structure. A reliable design with less weight and better dynamic performance was proposed. Hao and Liu (2017) carried out the evaluation of the anti-impact performance of OWT foundations due to head-on impact by ships. The damaged area, the maximum collision force, the maximum bending moment of the pile at the seabed, and the maximum steel consumption in different scenarios for OWT foundations were investigated and analyzed. Larsen (1991) used the single-moment spectral method for predicting the fatigue life of offshore structures subjected to complex loadings. Currently, most of the offshore wind turbine support structures are close to their half-designed lifetime, so for the maintenance and operation of offshore support structures, reassessing the remaining life is more important. Mai et al. (2019) proposed taking the oceanographic and strain data each year to predict the remaining fatigue life of wind turbine support structures. As the demand for renewable energy increases, the global cumulative installed capacity would also increase on large scale (Dong et al., 2012; Yeter et al., 2016; Nabuco et al., 2020; Mai et al., 2019). However, the tubular joints being fatigue sensitive are usually located in difficult access areas where maintenance and inspection are almost impossible. The development of an accurate and realistic FE method for predicting the fatigue life and crack initiation positions is necessary for extending the fatigue life of offshore wind turbine support structures. Many fatigue assessment methods were developed by researchers. One of them was the effective notch stress method which is highly recommended by the International Institute of Welding. In the effective notch stress method, the fatigue crack initiation period is not accurately predicted due to the already inclusion of a notch with a radius of either 0.05 mm or 1 mm in the specimen during fatigue assessments, which overall gives rise to uncertainties regarding the estimation of fatigue life and crack initiation positions. The prediction of the crack growth period is entirely different, depending on the different conditions of the material, geometry, and environment. In this study, 3D fatigue analysis based on constitutive equation and continuum damage mechanics was used to accurately predict initial fatigue cracks and estimate fatigue

life which incorporated both crack initiation periods. In the analysis, the initial welding state of tubular joints of offshore structures was reproduced to calculate the residual stresses and welding deformation. Latter was used as input along with external repeated loading to calculate the fatigue life and crack initiation positions. The S-N curve results obtained from fatigue analysis were compared with the S-N curve recommended by Eurocode 3 (Class 90 and Class 71). The 3D fatigue FE analysis is an effective tool for accurately predicting the crack initiation, and direction with the purpose to predict the remaining fatigue life of tubular joints of complex structures.

3. Procedure of FE Welding Analysis

Welding is the most important joining way in modern steel structures due to its advantage of connecting any shape of the structure, saving labor, steel, and time and having high production efficiency. The welded structures have occupied an absolute advantage in the present era in offshore, industrial as well as in civil building structures due to their elevated strength-to-weight ratio. The welding process involves the complex interaction of several mechanisms such as heat transfer, phase transformation, heat-affected zone (HAZ), welding deformation, residual stresses, etc. The presence of residual stresses and welding distortions in structures significantly affect fatigue behavior and durability under cyclic loading. To minimize the consequences and ensure high fabrication quality as well as high productivity, it is necessary to carefully control the welding residual stress and distortions. Currently, numerical simulations have become a powerful tool for industry to make improvements in the fabrication process and welding technology. Many approaches have been developed during the last decades, depending on the goal, and required preciseness of the FE simulation. The use of numerical simulation not only replaces the tedious trials and errors of digital processing technologies but also helps in significant cost reduction with increased product quality. Moreover, due to enhanced computational power, it is now feasible to analyze large-scale welded joints and complex engineering structures with great precision.

In this paper, the first welding process is reproduced using thermo-mechanical formulation. The thermal history of the weld is computed using a thermal analysis, which serves as input for the computation of residual stresses and welding deformation. The effect of 3D non-steady temperature analysis on the structural response is considered through the temperature-dependent mechanical and physical properties of the material. Simulation of welding is carried out using 3d-thermo mechanical analysis built on using in-house FE code, verified extensively against the numerical analysis in in-house FE code (Chang and Lee, 2006; Chang et al., 2011; Shin et al., 2021; Jang and Chang, 2008).

3.1 FE Welding Analysis Model

For fixed offshore structures, the circular hollow sections are considered the primary choice due to their characteristics like increasing structural efficiency in resisting harsh environmental loading conditions and minimizing the hydrodynamic forces. In complex offshore structures, the circular hollow sectional members are joined by welding. Two or more tubular members are welded together to form a connection referred to as a tubular joint. A tubular joint consists of different pipes with varying diameters, the smaller diameter pipes are called braces, and the larger one welded directly onto the surface braces is called a chord.

In this section, FE modeling of tubular joints of the tripod and

Table 1. Mechanical Properties of the Base and Weld Materials Used in FE Analysis

Material	E (GPa)	ν	σ_y (MPa)	σ_u (MPa)	Elongation (%)
SM490	206	0.3	344.3	580.0	30.6
GP Z312YGW11			490	570	30.0

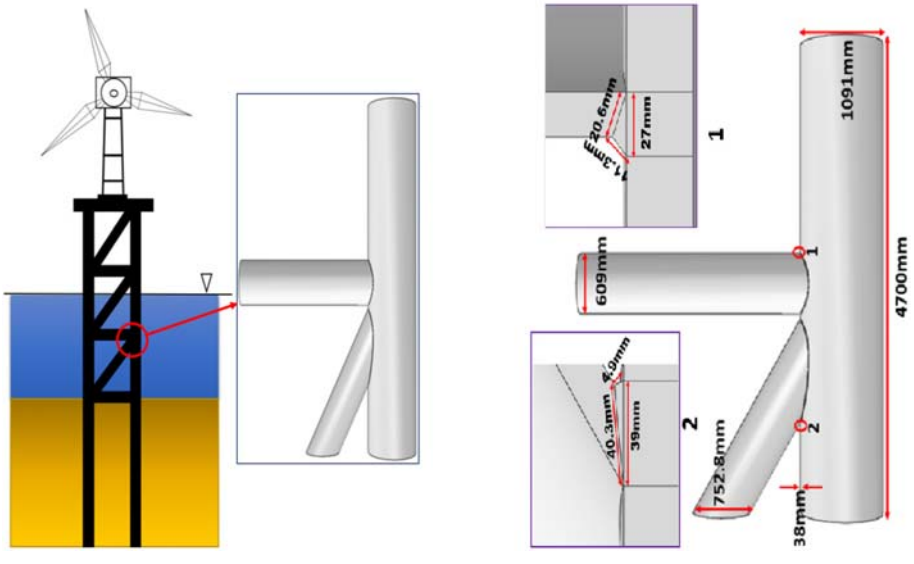

Fig. 1. Jacket Structure and Dimensions of Jacket Tubular Joint (TY type)

jacket support substructure was carried out. The tripod is a three-legged steel jacket support structure, the main part of the tripod is the central column, the lower part of which is connected to three legs and braces arranged in a triangular form. Whereas the jacket support structures are three-dimensional space frames consisting of vertical or battered legs supported by a bracing system. In both support substructures, the central column beneath the wind turbine transfers the load from the central tower to the inclined tubular members (legs), and the legs anchored in piles will transfer the load to the ground. The legs (tubular members) of the tripod and jacket support substructures were welded. A V-groove weld using girth-welding with full penetration at each joint was constructed. A full FE model of the upper tubular joint in tripod support structures was also considered. Fig. 1 shows the jacket support structure with a lateral bracing system and dimension of TY type tubular joint. Fig. 2 shows the three-legged tripod with chord and brace members. The dimensions of the tubular joints (DT and Y type) of the tripod structure are shown in Fig. 3. A fine mesh of about 1 mm was used near the close area of the weld to capture the stress gradients and deformations. The eight-noded isoparametric element was used as shown in Fig. 4. The size of the element increases progressively in both chord and brace members, with distance from the weld area. The Mesh view of the three tubular joints is displayed in Fig. 5.

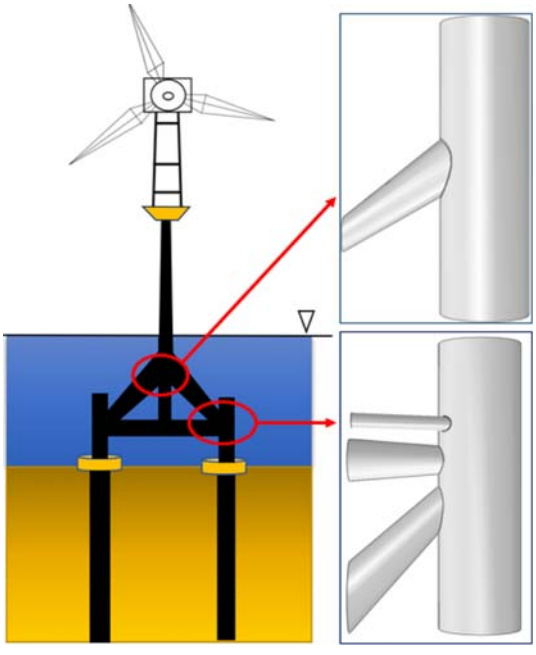

Fig. 2. Tripod Structure (DT type)

3.2 Welding Temperature and Thermal Elastoplastic Analysis

Nowadays, we use three-dimensional models in numerical analysis due to sufficient computing power. The analysis is divided into three parts first modeling and preparation of the material base, second calculation of temperature history, and third computing welding residual stresses and distortions. Accurate determination

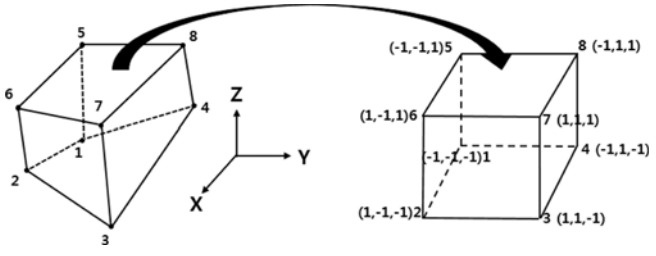

Fig. 4. The Eight-Noded Isoparametric Solid Element

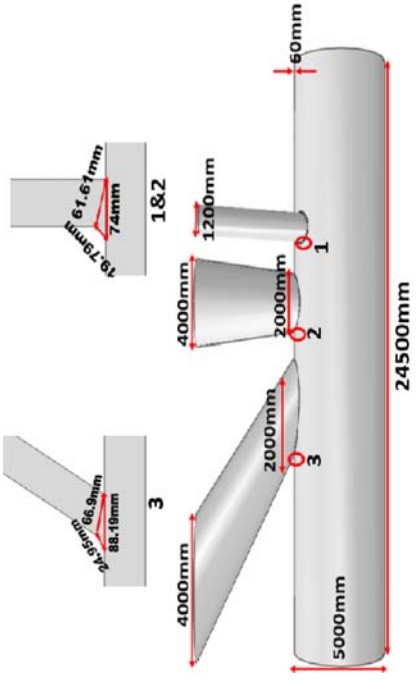

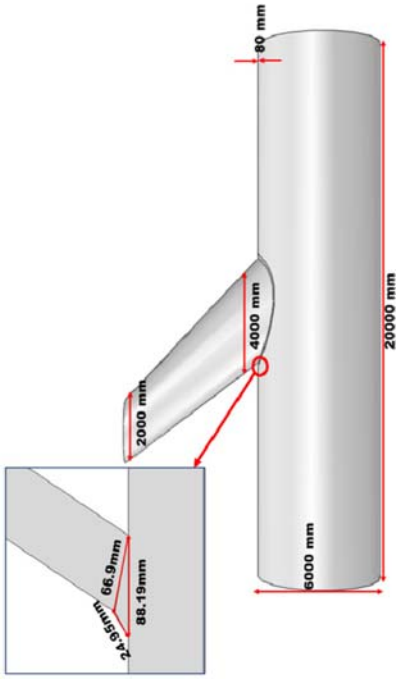

Fig. 3. Dimensions of Tripod Tubular Joints (Y type)

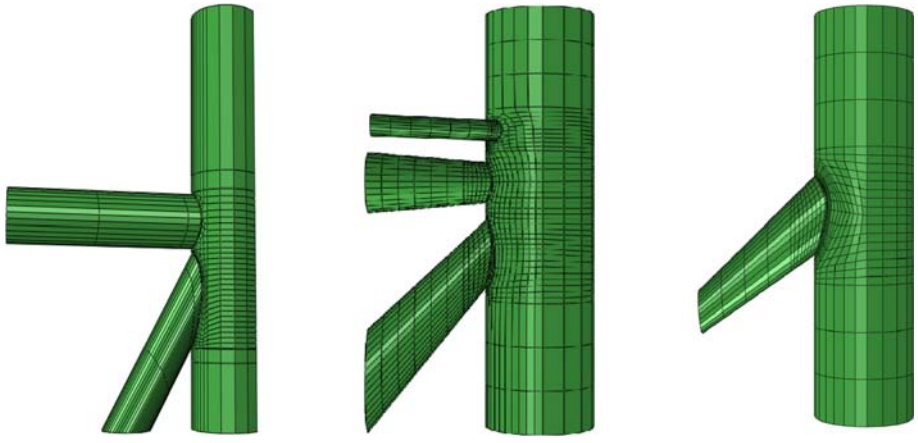

Fig. 5. Mesh View of Tubular Joints of Both Jacket and Tripod Structure

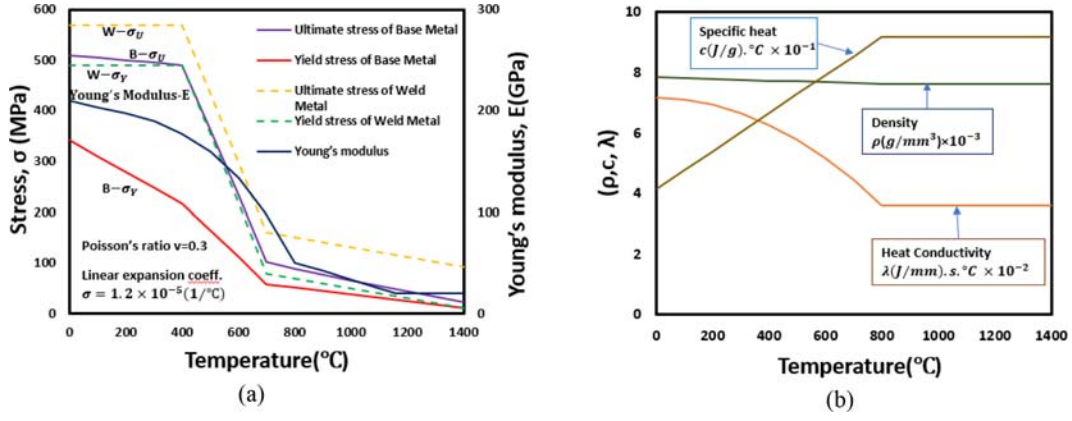

Fig. 6. Temperature-dependent Mechanical Material Properties and Physical Constants: (a) Mechanical Material Properties, (b) Physical Constants

of the temperature field and its influence on the material properties are the basic and important steps. During welding the transient heat transfer governing equation is given by

$$\rho c\frac{\partial T}{\partial t}(x,y,z,t) = -\nabla\cdot\vec{q}(x,y,z,t)+Q(x,y,z,t)\,. \tag{1}$$

The non-linear isotropic Fourier heat flux equation is governed as:

$$\vec{q} = -k\nabla T\,. \tag{2}$$

In the combined heat source model, the heat of the welding arc is designed by a Gaussian distributed surface heat source, and the heat of melting droplets is modeled by a volumetric heat source with uniform density. The heat flux distribution at any time, within r_0 on the surface of the workpiece is governed by the following equation.

$$Q(t) = \frac{3Q_A}{\pi r_0^2}\exp\left[-\left(\frac{r(t)}{r_0}\right)^2\right] \tag{3}$$

In welding simulation, for boundary conditions, heat loss is generally considered by using Newton's law of cooling and Stefan-Boltzmann's law. In the subsequent thermo-mechanical analysis, the temperature history of each node computed by the preceding heat transfer analysis for each time step increment is induced as input (thermal load) for calculating the residual stress and welding deformations in mechanical analysis. The thermal history graph for three tubular joints is shown in Fig. 7. The equilibrium and constitutive equations were used in the mechanical analysis. In addition, during the welding process in mild steels, the solid-state phase transformation has an insignificant effect on welding deformation and welding residual stress. So, additive strain decomposition is used to decompose the total strain rate into three components as follows:

$$\{d\varepsilon_{ij}\} = \{d\varepsilon_{ij}^{e}\}+\{d\varepsilon_{ij}^{p}\}+\{d\varepsilon_{ij}^{th}\}\,. \tag{4}$$

The components $d\varepsilon_{ij}^{e}$, $d\varepsilon_{ij}^{p}$, $d\varepsilon_{ij}^{th}$ correspond to elastic, plastic, and thermal strain increments respectively. The isotropic Hook's law with temperature-dependent physical constants is used to calculate the elastic strain, the plastic strain rate is modeled using the Von Mises yield criterion, and the temperature-dependent mechanical properties and isotropic hardening and thermal strain rate are computed using the coefficient of thermal expansion. The same finite element model from thermal analysis, with the same mesh size except for element type, was used to enhance data mapping and convergence during structural analysis. The element type has one degree of freedom i.e., the temperature at each node in thermal analysis whereas in mechanical analysis the element type has three translational degrees of freedom at each

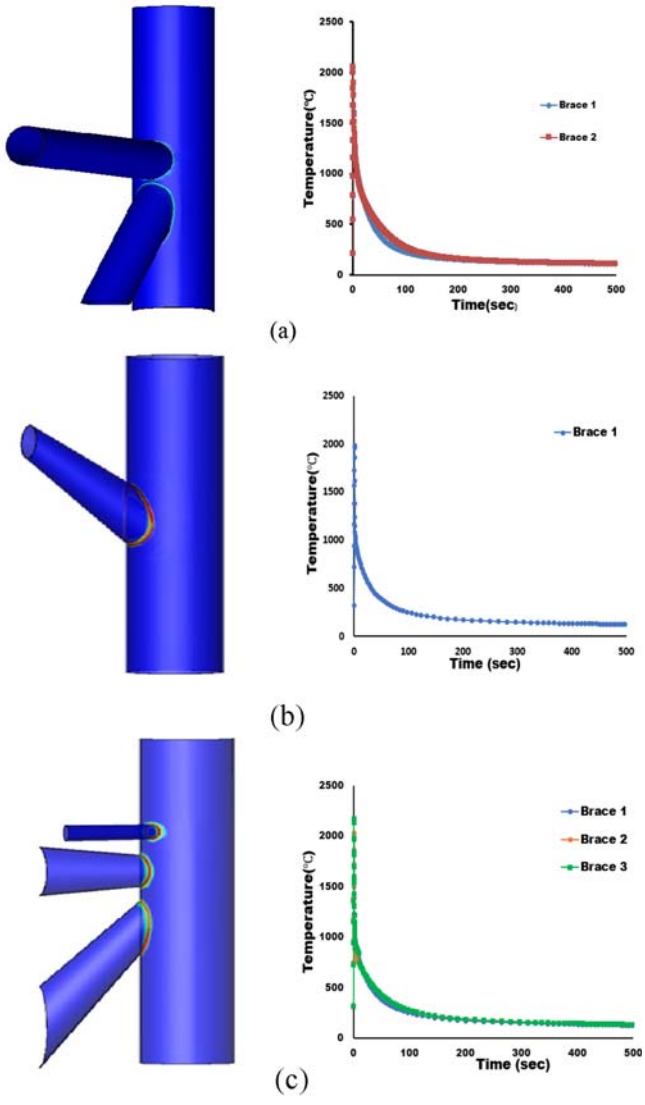

Fig. 7. Temperature Distributions: (a) Temperature Distributions in Tubular Joint (TY type) of Jacket Structure, (b) Temperature Distributions in Upper Tubular Joint (Y type) of Tripod Structure, (c) Temperature Distributions in Lower Tubular Joint (DY type) of Tripod Structure

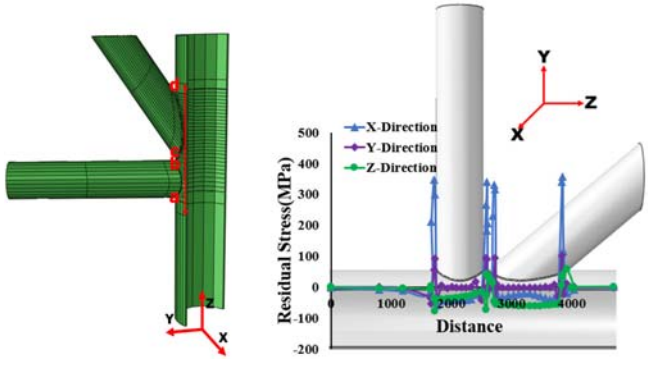

Fig. 8. Residual Stress Distribution in Tubular Joint of Jacket Structure

node. In thermal and mechanical analysis, a full Newton-Raphson iterative solution was employed to incorporate the behavior of rapidly changing temperature-dependent material properties and

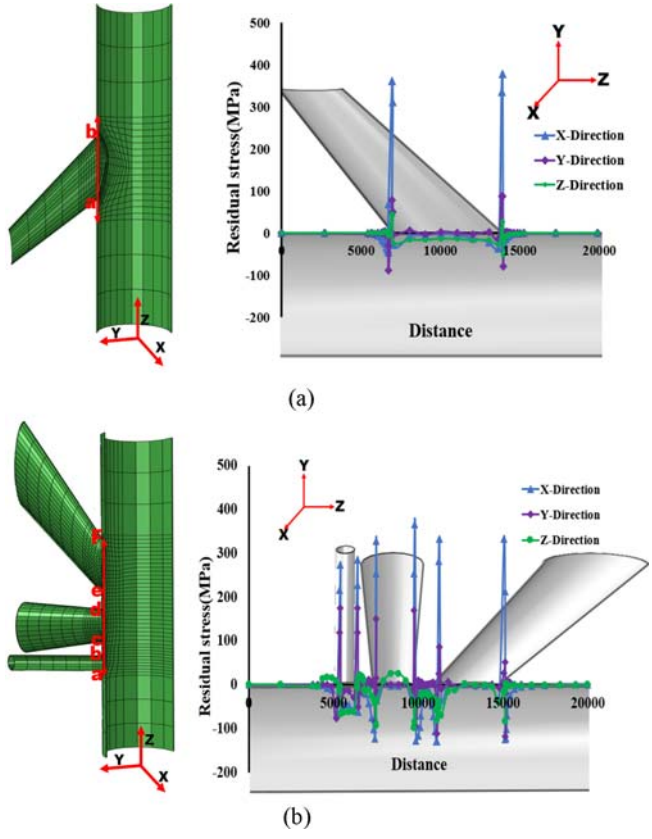

Fig. 9. Residual Stress Distribution: (a) Residual Stress Distribution in Upper Tubular Joint of Tripod Structure, (b) Residual Stress Distribution in Lower Tubular Joint of Tripod Structure

temperature as shown in Fig. 6. The mechanical properties of the base metal and the weld metal are given in Table 1. The stiffness matrix after every equilibrium iteration is reformulated with modified material properties to give accurate results (Chang et al., 2011; Chang and Lee, 2006; Shin et al., 2021). The residual stress graph for the TY-type tubular joint of the jacket support structure is shown in Fig. 8. And the residual stress graph for tubular joints (DT and Y type) of the tripod support structure is shown in Fig. 9. In all three tubular joints, the maximum tensile residual stresses developed in circumferential directions.

4. Fatigue FE Analysis for DK-type Joint of Tripod Structure

Fatigue failure is one of the most dominant mechanical failures in structures. Fatigue failure is affected by several parameters such as surface roughness, stress values, size of structural components, stress gradients, etc. Therefore, the accurate assessment of the reliability of structures and correct evaluation of damage accumulation under different loading histories are important. Fatigue failure is divided into three stages: crack initiation, crack propagation, and complete rupture. For components without initial material and geometrical imperfection, the crack initiation phase usually accounts for more than 80% of the total fatigue

Table 2. Damage Model Parameters for the Isotropic and the Kinematic Hardening Rates

Material	c_1	c_2	c_3	γ_1	γ_2	γ_3	Q	b
SM490	130.0	85.0	1.271	300.0	56.67.	1.0	75.0	18.27

life. The study of crack initiation for structural components in service is of great significance. A lot of models have been developed by different researchers to predict the crack initiation and fatigue life but due to a lack of adequate methodology, they were unable to estimate internal damages that occurred prior to crack initiation and also could not simulate the crack propagation in the weld part. Continuum damage mechanics is regarded as the effective method to study crack initiation, propagation, and material stiffness degradation and accurately predict the total fatigue life (Chaboche and Lesne, 1998; Lemaitre, 1985; Zhang et al., 2012; Vuong NVD et al., 2015a; Vuong NVD et al., 2015b; Muzaffer et al., 2022).

In this study, a non-linear damage cumulative model for multiaxial high-cycle fatigue was used based on CDM using the internal FE-code to simulate the fatigue loading and the FE code has been verified extensively. Using FE techniques, the fatigue damage model was applied to weld induced FE model to predict the fatigue life and crack initiation positions. The fatigue damage model material parameters for the base material (SM490) are given in Table 2.

Under cycling loading, material properties deteriorate continuously, and the damage variable is dependent on the size of stress and strain. The fatigue damage model estimates the advancement of damage value at a material point and calculates lifetime in terms of the number of cycles. The analysis is fully coupled considering the interactions between the elastic-plastic material behavior and damage level of all reference elements during the entire process. The set of constitutive equations for a particular material can be formulated by the thermodynamics of irreversible phenomena through a certain number of variables called state variables. A few sets of state variables are always taken into consideration while calculating the damage that involves both elastic and plastic strain. Using the generalized normality rule, from the state and dissipation potential for damaged material and the decomposition of strain rates, the constitutive set of equations are written as follows:

$$\dot{\varepsilon}_{ij}^{t} = \dot{\varepsilon}_{ij}^{e} + \dot{\varepsilon}_{ij}^{p}. \tag{5}$$

The elastic strain is given by:

$$\dot{\varepsilon}_{ij}^{e} = \frac{1+\nu}{E}\frac{\dot{\sigma}_{ij}}{1-D} - \frac{\nu}{E}\frac{\dot{\sigma}_{kk}}{1-D}\delta_{ij}. \tag{6}$$

The plastic dissipation potential from the plasticity theory with Von Misses yield criterion was obtained as:

$$F_p(\bar{\sigma}, X, R, D) = \sigma_{eq} - R(p) + \sigma_y + \frac{3}{4X_\infty}X_{ij}^{D}X_{ij}^{D}. \tag{7}$$

σ_{eq} is the equivalent of Von Mises stress.

The plastic strain rate using the normality rule obtained from the plastic dissipation potential:

$$\dot{\varepsilon}_{ij}^{p} = \dot{\lambda}\frac{\partial F_p}{\partial \sigma_{ij}} = \frac{3}{2}\frac{\dot{\lambda}}{1-D}\frac{\frac{\sigma_{ij}^{D}}{1-D} - X_{ij}^{D}}{\sigma_{eq}}. \tag{8}$$

$\dot{\lambda}$ is the plastic multiplier.

The internal variables associated with the kinematic hardening rate (X_{ij}) and isotropic hardening rates (R) are as follows:

$$\dot{X}_{ij}^{D} = \sum_{K=1}^{n}(\dot{X}_{ij}^{D}) = \sum_{K=1}^{n}\gamma_k\left(\frac{2}{3}c_k\dot{\varepsilon}_{ij}^{p} - (X_{ij}^{D})_k\dot{p}\right) \tag{9}$$

$$\dot{r} = q(b\cdot e^{-bp})\dot{p} \tag{10}$$

where n is the number of back stresses, c_k and γ_k are constant values obtained from cyclic loading for every back stress evolution, and Q and b are material constants associated with isotropic hardening and calculated from fully reversed strain-controlled testing. It is necessary to specify the damage dissipation potential to complete the set of constitutive equations. The damage evolution rate is expressed as:

$$\dot{D} = -\dot{\lambda}\frac{\partial F_D}{\partial_x} = -\frac{\partial \phi^*}{\partial_x}. \tag{11}$$

Combining the above FEA with damage mechanics, to calculate the remaining life and crack initiation of structure. In the proposed fatigue damage model, the damage evaluation is done in terms of the remaining lifetime and by using the effective stress concept. For uniaxial loading the damage growth differential equation proposed by Chaboche is written as:

$$\delta D = [1-(1-D)^{\beta+1}]^{\alpha(\alpha_{Max},\bar{\sigma})}\left[\frac{\sigma_{Max}-\sigma_m}{M(\sigma_m)(1-D)}\right]^{\beta}\delta N. \tag{12}$$

The Number of cycles to microscopic crack initiation obtained by integrating the above equation:

$$N_F = \frac{1}{(\beta+1)[1-\alpha(\alpha_{Max},\bar{\sigma})]}\left(\frac{\sigma_{Max}-\sigma_m}{M_{(\sigma_m)}}\right)^{-\beta}. \tag{13}$$

The welded structure under cyclic loading with the weld-induced residual stresses is subjected to multiaxial fatigue presenting a complex path during the loading cycle. A fatigue limit criterion (f_F) was introduced to take into consideration the multiaxial stress character

$$f_F = A_\pi - A_\pi^*$$

where A_π is defined in proportional loading and A_π^* is the Sines fatigue limit criterion (Vuong et al., 2015a; Vuong et al., 2015b). The 3D fatigue damage model was obtained using one-dimension law describing the damage evolution in uniaxial and the effect of nonlinear accumulation a 3D criterion of fatigue guides the choice of the significant stress invariants in the law, so for the 3D stress state the evolution of fatigue damage is expressed as:

$$\delta D = [1-(1-D)^{\beta+1}]^{\alpha(\alpha_{Max},\alpha_m)}\left[\frac{A_\pi}{M(\sigma_m)(1-D)}\right]^{\beta}\delta N \tag{14}$$

Under constant amplitude loading, integrating the above equation between $D = 0$ and $D = 1$ gives the number of cycles for rupture.

$$N_f = \frac{1}{(\beta+1)(1-\alpha)}\left(\frac{A_n}{M(\sigma_m)}\right)^{-\beta} \quad (15)$$

The damage calculation is done in incremental form:

$$D_{N+\Delta N} = D_N + \Delta D \quad (16)$$

The iterative method was used for the repetition of the analysis. The damage value accumulates with time and when reaches the critical value at any specific element causing the stiffness of the specific element to be zero. Simultaneously the whole system gets updated, and the iterations kept running until the crack propagates through the entire weld length leading to the rupture of the structure. The number of iterations terminated at the occurrence of the first crack was determined as the fatigue life of the weld under repeated loading.

4.1 Load and Boundary Condition of 3D Fatigue FEA

In the high cycle, multiaxial damage model, the geometries, and material were the same as in the previous residual analysis except for boundary and loading conditions. The mesh distribution was also similar in order to enhance data mapping easily between the two structural models. Eight node isoparametric elements were used with three degrees of freedom at each node. The welding deformation and residual stresses calculated from the mechanical analysis were given as input into the model. The cyclic fatigue loading was applied as displacement on the top of braces in the Y-direction as shown in Fig. 10(b). In order to determine the fatigue life, a high cycle fatigue damage model based on internal FE-code was used to simulate fatigue loading tests. The boundary conditions on the three FE models were applied, with one end of the chord fully fixed by restraining all the moments and displacements while roller support was given at the other end of the chord as displayed in Fig. 10(a). All the nodes at top of the brace were kinematically coupled for translation in a direction similar to the applied load. The red line on the braces indicate loading was applied on all the nodes and red arrow shows the direction of loading similarly the black rings at the end of chord member shows all the nodes on either side of chord member were constrained in different directions.

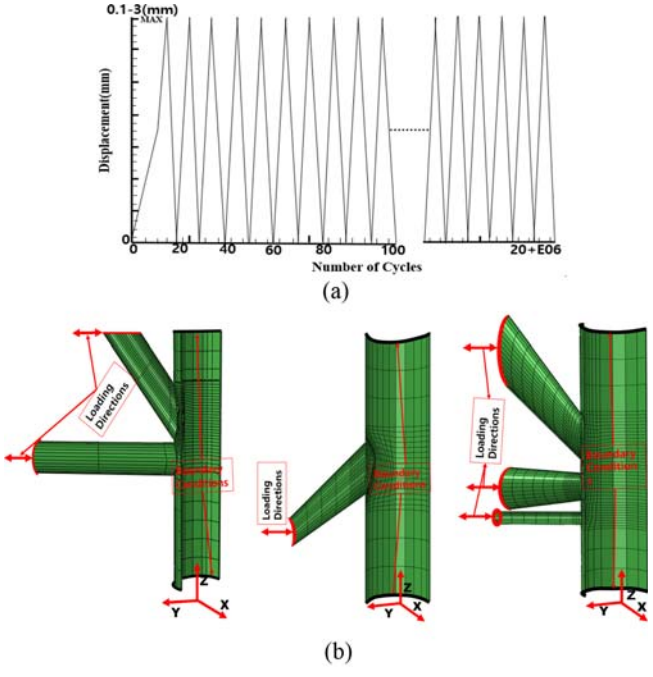

Fig. 10. Loading Direction and Boundary Conditions: (a) Cyclic Load Type, (b) Boundary and Loading Conditions

5. Results and Discussion

5.1 Comparison of Fatigue FEA Results with Eurocode 3

Multiaxial fatigue helps in providing a better understanding of the risks associated with an in-service issue and therefore the ability to go on to redefine the safety limits to enable a better design. The fatigue evaluation of the structure under multiaxial loading is a very complex behavior so in this study, multiaxial cyclic stress was reduced to equivalent cyclic stress to account for the effect of loadings, shear and tensile stresses on fatigue life and the results can be easily compared with uniaxial stresses. The S-N curve describes a relation between equivalents stress and the number of cycles. On the horizontal axis, the number of cycles to failure is given on a logarithmic scale, and on the vertical axis, the equivalent stress range with a logarithmic scale is given. The S-N curve of all three tubular joints considering weld-induced residual stresses and deformation under constant amplitude loading is shown in Figs. 11 and 12. In some loading cases, the analysis was stopped after the number of cycles was greater than 2 million.

Figure 11 shows the comparison of fatigue life for two joints at the same stress ranges and determined that the fatigue life of the lower joint (DY type) of the tripod support structure is

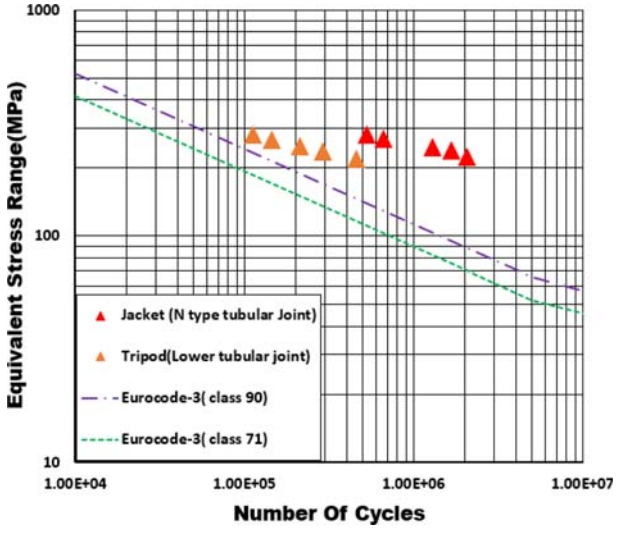

Fig. 11. Comparison of Results from Fatigue FEA, with Eurocode 3 for Lower Joint of Tripod and TY-tYpe Joint of Jacket Structure

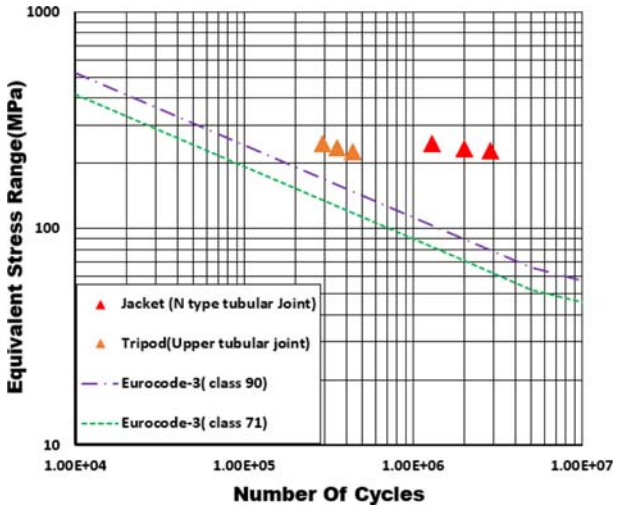

Fig. 12. Comparison of Results from Fatigue FEA, with Eurocode 3 for the Upper Joint of the Tripod and the TY-Type Joint of the Jacket Structure

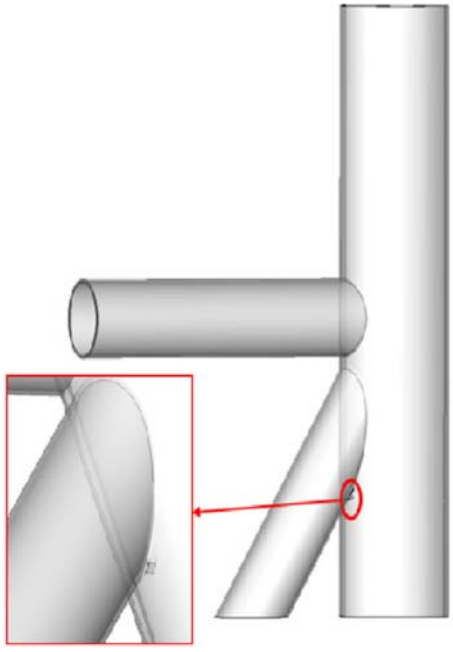

Fig. 13. Crack Initiation Position in N-Type Tubular Joint

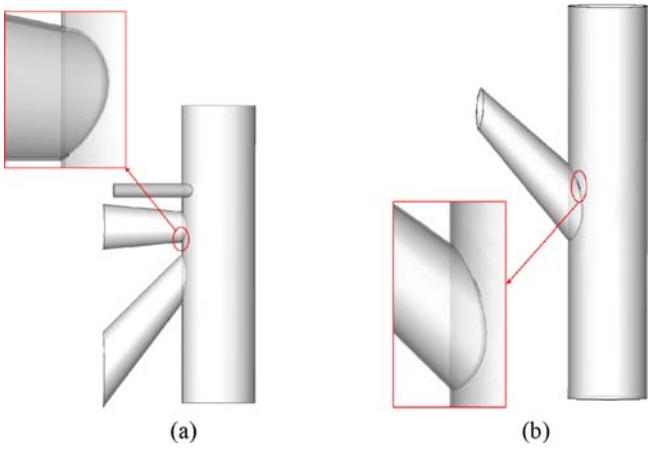

Fig. 14. Crack Initiation Position in Tubular Joints of Tripod Support Structure: (a) Crack Initiation at Lower Joint of Tripod Structure, (b) Crack Initiation at N-Type Joint of Tripod Structure

shorter compared to the (TY type) joint of the jacket support structure. Fig. 12 compared the fatigue life of the upper joint (Y type) of the tripod support structure and the same TY type joint of the jacket support structure at the same stress range from S-N curves it was predicted that the fatigue life of the TY type tubular joint of the jacket support structure is greater than the tubular joints of the tripod support structure. It was depicted from the results the jacket support structure has more long fatigue life compared to the tripod support structure. So, lattice-type support structures like jacket support structures are considered the best support structure due to their great structural stiffness, lightweight, less damage area, and better modal performance. The construction of a tripod support structure is very troublesome due to the large diameter of the central column. Also, the presence of ovality i.e., deviation from perfect circularity makes load distribution complicated which results in lesser fatigue life compared to the jacket support structure.

5.2 Crack Initiation

Fatigue crack initiation is a complex phenomenon that is influenced by many interacting parameters. When the local stress exceeds the yield strength of the material, thereby plastic displacements occur, and accumulation of these plastic displacements leads to the creation of micro-cracks that grows with time under the applied cyclic loads. A crack presented in the damage model is defined as a region of completely damaged material. In this region, complete loss of stiffness implies that the stresses in this region are identically zero for arbitrary deformation fields. The beginning of crack propagation is at the point when total force drops to zero and failure of structure rapidly changes about the small number of cycles. In the initial stage, the damage growth is relatively small, and its evolution is gradually increasing, damage variable also changes faster leading to the first failure in the element i.e., crack initiation which with time under continuous cyclic loading can propagate throughout the whole weld finally leading to the rupture of the structure. The presence of higher tensile residual stresses at the welded toe in all the three welded tubular joints also amplifies the crack initiation. The residual stresses superpose with the internal stresses generated by external loading, so the total stresses developed will be higher than yield stress. The stress-strain behavior gets updated after every cycle and damage variable get accumulated until it reaches a critical value leading to the crack initiation in structure. The crack initiation in the TY type tubular joint of the jacket support structure occurred at the crown of an inclined brace as shown in Fig. 13. The crack initiation in the lower tubular joint (DY type) of the tripod support structure appeared at the crown toe of the perpendicular brace as displayed in Fig. 14(a) whereas, in the upper joint (Y type) of the tripod support structure, the crack

initiation emerged in the region between saddle and crown of incline brace as presented in Fig. 14(b). If high tensile residual stress exists near the weld end of the TY-type tubular joint of the jacket support structure and near the weld end of the tubular joint of the tripod support structure, it overlaps with the internal stress caused by the external load, which accelerates the damage accumulation leading to the crack initiation. Ultimately, the fatigue life of welded tubular joints is significantly reduced.

6. Conclusions

This paper presented an investigation into the fatigue life and crack initiation positions of tubular joints of the jacket support structure and tripod support structure. In this study, the effect of residual stress and welding deformation in conjugation with external repeated loading on fatigue life was considered. Based on the comparisons of the results the following conclusions were drawn from this work which are summarized in the following points:

1. The welding residual stress and welding deformation affect the fatigue life and crack initiation.
2. The fatigue life of tubular joints (TY type) in jacket support structures has almost 20% more fatigue life compared to the lower tubular joints (DT type) in tripod support structure and when the same tubular joint (TY type) of jacket structure was compared with the Y-type tubular joint of tripod support structure, the fatigue life of Y type tubular joint in tripod structure demonstrates a 11.4% increase in fatigue life than the TY type tubular joint in jacket structure.
3. The crack initiation positions in all three tubular joints were predicted. The crack initiation in TY type tubular joint in jacket structure and in Y-type joint in tripod structure occurred at the weld toe of the inclined member whereas the crack initiation in DT type tubular joint (lower joint) occurred at the weld toe of perpendicular brace.
4. The 3D fatigue FE analysis data were compared with the S-N Curves recommended by Eurocode3. From results it was proven that the fatigue FE analysis method is reliable method.

Acknowledgments

This research was supported by the Basic Science Research Program through the National Research Foundation of Korea (NRF) funded by the Ministry of Education (NRF-2021R111A204584511). This research was also supported by Chung-Ang University research grants in 2018.

Nomenclature

A_n = Amplitude of octahedral shear Stress
c = Specific heat
D = Damage variable
D_N = Damage value at Nth cycle
k = Thermal conductivity
N = Number of cycles
N_f = Number of cycles to failure
Q = Rate of moving heat generation per unit volume
Q_A = Heat input from the welding arc
Q, b = Material constants in isotropic hardening rate function
R = Isotropic hardening rate
ro = Arc beam radius
X_{ij}^{D} = Back stress increment tensor
α, β = Material constants of damage
∇ = Spatial gradient operator
ΔD = Increment of damage evolution
δN = Increment of the number of cycles
$\overline{\sigma}$ = effective stress tensor
$d\varepsilon_{ij}$ = Total strain increment
$d\varepsilon_{ij}^{p}$ = Elastic strain increment
$d\varepsilon_{ij}^{p}$ = Plastic strain increment
$d\varepsilon_{ij}^{th}$ = Thermal strain increment
γ_k, c_k = Material constants in kinematic hardening
σ_{eq} = Equivalent of von Mises stress
σ_{ij} = Stress tensor
σ_m = Mean stress.
σ_{max} = Maximum stress
ρ = Density

ORCID

Not Applicable

References

Afandi AA, Muis Alie MZ (2020) Fatigue life Prediction on jacket leg structure subjected to axial and wave loads. *IOP Conf. Series: Earth and Environmental Science* 575:012194, DOI: 10.1088/1755-1315/575/1/012194

Ashuri T, Zaaijer MB (2007) Review of design concepts, methods, and considerations of offshore wind turbines. European Offshore Wind conference and exhibition, Berlin., Dec.

Chaboche JL, Lesne PM (1998) A non-linear continuous fatigue damage model. *Fatigue & Fracture of Engineering Materials & Structures* 11:1-17, DOI: 10.1111/j.1460-2695.1988. tb01216.x

Chang KH, Lee CH (2006) Characteristics of high-temperature tensile properties and residual stresses in weldments of high strength steels. *Materials Transactions* 47:348-354, DOI: 10.2320/matertrans.47.348

Chang KH, Lee CH, Park K, Um TH (2011) Experimental and numerical investigation on residual stresses in a multi-pass butt-welded high strength SM570-TMCP steel plate. *International Journal of Steel Structures* 11:315-324, DOI: 10.1007/s13296-011-3006-y

Chella AM, Tørum A, Dag M (2012) An overview of wave impact forces on offshore wind turbine substructures. *Energy Procedia* 20:217-226, DOI: 10.1016/j.egypro.2012.03.022

Chew KH, Muskulus M, Zwick D, Ng EYK, Tai K (2013) Structural optimization and parametric study of offshore wind turbine jacket substructure. Proceedings of the International Offshore and Polar Engineering Conference, ISSN 1098-6189

Chew K-H, Ng E, Tai K (2014) Offshore wind turbine jacket substructure: A comparison study between four-legged and three-legged designs.

Journal of Ocean and Wind Energy (ISSN2310-3604) 2:74-81, https://hdl.handle.net/10356/100546

Dong W, Moan T, Gao Z (2012) Fatigue reliability analysis of the jacket support structure for offshore wind turbine considering the effect of corrosion and inspection. *Reliability Engineering & System Safety* 106:11-27, DOI: 10.1016/j.ress.2012.06.011

Hao E, Liu C (2017) Evaluation and comparison of anti-impact performance to offshore wind turbine foundations: Monopile, tripod, and jacket. *Ocean Engineering* 130:218-227, DOI: 10.1016/j.oceaneng.2016.12.008

Henderson A, Zaaijer M, Camp T (2003) Hydrodynamic Loading of Offshore Wind Turbines. OWEMES Conference, Naples

Jang GB, Chang KH (2008) A rate-independent hysteresis model for structural steel (SM490) considering the coupled effect of strain rate hardening and temperature rise. *Materials Science Forum* 580-582, DOI: MSF.580-582.581

Kharade AS, Kapadiya SV (2014) Offshore engineering: An overview of types and loadings on structure. *International Journal of Structural and Civil Engineering Research* 2(3), ISSN 2319-6009

Larsen CE (1991) Predicting the fatigue life of offshore structures by the single-moment spectral method. *Probabilistic Engineering Mechanics* 6(20):96-108, DOI: 10.1016/0266-8920(91)90023-W

Lemaitre J (1985) A continuous damage mechanics model for ductile fracture. *Journal of Engineering Materials and Technology* 107:83-89, DOI: 10.1115/1.3225775

Mai QA, Weijtjens W, Devriendt C, Morato PG, Rigo P, Sorensen JD (2019) Prediction of remaining fatigue life of welded joints in wind turbine support structures considering strain measurement and joint distribution of oceanographic data. *Marine Structures* 66:307-322, DOI: 10.1016/j.marstruc.2019.05.002

Mendes P, Correia Jose AFO, Mourao A, Pereira R, Fantuzzi N, De jesus A, Calcada R (2021) Fatigue assessment of a jacket-type offshore structure based on static and dynamic analysis. *Practical Periodical on Structural Design and Construction* 26:04020054-13, DOI: 10.1061/%28ASCE%29SC.1943-5576.0000533

Muzaffer S, Chang KH, Wang ZM, Kang SU (2022) Comparison of stiffener effect on fatigue crack in KT-type pipe joint by FEA. *Weld World* 66:783-797, DOI: 10.1007/s40194-022-01254-z

Nabuco B, Tarpo M, Tygesen UT, Brinker R (2020) Fatigue stress estimation of an offshore jacket structure based on operational modal analysis. *Shock and Vibration*, Article ID: 7890247, DOI: 10.1155/2020/7890247

Oh KY, Nam W, Ryu MS, Kim JY, Epureanu BI (2018) A review of foundations of offshore wind energy converters: Current status and future perspectives. *Renewable and Sustainable Energy Reviews* 88:16-36

Plodpradit P, Dinh VN, Kim K-D (2019) Tripod-supported offshore wind turbines: Modal and coupled analysis and a parametric study using X-SEA and FAST. *Journal of Marine Science and Engineering* 7(6):181, DOI: 10.3390/jmse7060181

Sadeghi K (2007) An overview of design, analysis, construction, and installation of offshore petroleum platforms suitable for Cyprus Oil/gas fields. *International Journal of Steel Structures* 2(4):1-16

Shin WS, Chang KH, Shazia M (2021) Fatigue analysis of cruciform welded joints with weld penetration defects. *Engineering Failure Analysis* 120, DOI: 10.1016/j.engfailanal.2020.105111

Stahlmann A, Schlurmann T (2010) Physical modeling of scour around tripod foundation structures for offshore wind energy. *Coastal Engineering* 1(32), DOI: 10.9753/icce.v32.sediment.67

Vuong NVD, Lee CH, Chang KH (2015a) A constitutive model for uniaxial/multiaxial ratcheting behavior of duplex stainless steel. *Materials & Design* 65:1161-1171, DOI: 10.1016/j.matdes.2014.08.046

Vuong NVD, Lee CH, Chang KH (2015b) High cycle fatigue analysis in presence of residual stresses by using a continuum damage mechanics model. *International Journal of Fatigue* 70:51-62, DOI: 10.1016/j.ijfatigue.2014.08.013

Yang H-Z, Zhu Y, Lu Q, Zhang J (2015) Dynamic reliability-based design optimization of the tripod sub-structure of offshore wind turbines. *Renewable Energy* 78:16-25, DOI: 10.1016/j.renene.2014.12.061

Yeter B, Garbatov Y, Soares CG (2016) Evaluation of fatigue damage model predictions for fixed offshore wind turbine support structures. *International Journal of Fatigue* 87:71-80, DOI: 10.1016/j.ijfatigue.2016.01.007

Zaaijer MB (2003) Comparison of monopile, tripod, suction bucket, and gravity base design for a 6-MW turbine. Offshore Wind energy in Mediterranean and Other European Seas (OWEMES conference), Naples, Italy, April 2003

Zhang L, Liu X, Wang L, Wu S, Fang H (2012) A model of continuum damage mechanics for high cycle fatigue of metallic materials. *Transactions of Nonferrous Metals Society of China* 22:2777-2782, DOI: 10.1016/S1003-6326(11)61532-X